Visible intracavity laser spectroscopy with a step-scan Fourier-transform interferometer

Kimberly Strong, Timothy J. Johnson, and Geoffrey W. Harris

A Fourier-transform spectrometer has been used in a step-scan mode to make time-resolved measurements of the evolving laser pulse in intracavity laser spectroscopy (ILS) experiments. Spectra of broadband dye laser pulses at approximately 615 nm were recorded at relatively high spectral (0.5-cm^{-1}) and temporal (as high as 5-μs) resolution. In the absence of an absorber, the height of the pulse is shown to be proportional to $t_g^{0.57}$ (where t_g is the generation time) for generation times as high as 500 μs. The system was constructed for feasibility studies of future use at infrared and near-infrared wavelengths where conventional ILS that uses diode arrays would be either expensive or simply not possible. The CH_4 overtone transition at 619.68 nm was used to test the linearity and sensitivity of the system. Comparable performance to conventional ILS systems was demonstrated, as were the advantages of the present system for studies of laser and absorption dynamics. © 1997 Optical Society of America

Key words: Intracavity laser spectroscopy, step-scan Fourier-transform interferometry, time-resolved spectroscopy.

1. Introduction

Several approaches are available to achieve time-resolved observations of fast phenomena by use of spectroscopic techniques. Many approaches follow a generalized scheme with a trigger (often a light pulse), followed by a fixed delay and a diagnostic process, which can involve either the collection of emitted or scattered photons or the absorption of photons from a (second) incident beam. Especially in emission studies, the diagnostic photons are often dispersed by a grating instrument to determine spectral distribution. Excellent temporal resolution can be obtained with such methods[1]; however, investigation of the time dependence of the phenomena is possible only by one changing the delay time and repeating the experiment. Fourier-transform (FT) techniques are broadband and exhibit a higher throughput compared with dispersive systems,[2] but conventional FT spectrometers are limited in the time resolution that they can achieve by the speed at which the interferometer moving mirror can be translated. Temporal resolution usually can be obtained by a comparison of two successive spectra, i.e., two successive mirror scans, and the fastest conventional interferometers can acquire only ~50 spectra s^{-1} even at low (8-cm^{-1}) spectral resolution.

Step-scan FT spectrometers obtain high temporal resolution in a different manner.[3] With these instruments, the moving mirror is translated (stepped) to a fixed position so that the optical path difference remains temporarily constant. An experiment is then initiated (e.g., a photochemical reaction is triggered by a light pulse), and the interferogram intensity at that mirror position is digitized at equispaced time intervals (e.g., every 5 μs). The mirror is then stepped to the next position, the experiment is triggered again, and a new set of fixed-retardation intensities is recorded. The process is repeated until the time-varying intensities are recorded for a complete set of mirror positions. At the conclusion, the two-dimensional matrix is rotated into a series of retardation-spaced intensities (i.e., interferograms) for different times, each interferogram corresponding to a given time after trigger. The interferograms are then Fourier transformed successively into a series of spectra, each corresponding to a selected delay time relative to the triggers. The temporal resolution is thus limited only by the detector and digitizer (analog-to-digital converter) bandwidths.

There have been several reports on the use of step-

When this research was undertaken, all the authors were with the Centre for Atmospheric Chemistry, York University, 4700 Keele Street, North York, Ontario M3J 1P3, Canada. K. Strong is currently with the Department of Physics, University of Toronto, 60 St. George Street, Toronto, Ontario M5S 1A7, Canada. T. J. Johnson is currently with Bruker Optics, 19 Fortune Drive, Billerica, Massachusetts 01821.

Received 4 March 1997; revised manuscript received 21 July 1997.

0003-6935/97/338533-08$10.00/0

scan time-resolved spectroscopy (TRS) emission experiments since the first research by Biggs *et al.*[3] and Hancock and Heard,[4] who constructed an instrument to monitor infrared emissions from chemiluminescent systems such as O + CF_2. These reports include the demonstration of very fast (nanosecond) temporal resolution.[5,6] Hartland *et al.*[7] have investigated the energy levels of species such as CH_2 by monitoring the high-resolution emission spectra of the photolytically generated radicals. There are fewer reports of step-scan TRS absorption experiments; Johnson *et al.*[8] described a study of gas-phase kinetics using a laser flash photolysis system coupled with TRS, and Uhmann *et al.*[9] studied time-resolved absorptions in bacteriorhodopsin systems. Recently, others have undertaken TRS studies of similar biochemical systems, in particular Hage *et al.*,[10] as well as Plunkett *et al.*[11] The technology is rapidly becoming more accessible, and the number of step-scan TRS studies is expected to grow.

The first two reports of intracavity laser spectroscopy (ILS) appeared independently over 25 years ago.[12,13] Despite the difficulty of rigorous theoretical interpretation of the effect, the main features of ILS can be described in a simple way: A lasing medium with a broadband gain characteristic (e.g., a dye laser) is pumped discontinuously by a chopped cw source; the dye laser reaches threshold, and in the absence of a tuning element, several different cavity modes begin to oscillate, yielding an emission with a relatively broad spectral distribution. As time progresses, mode competition sets in, and certain modes within the cavity are enhanced relative to the others, leading eventually to a cw line that is relatively narrow. The total time elapsed between the start of lasing in the broadband medium and the stabilization of the spectral evolution of the developing cw emission is a function of the laser, the cavity length, the pump power, and several other factors that are for the most part not fully understood. For commercially available dye lasers such as the one we used for our research, typical parameters can be an initial pulse width of 4.0 nm ($\sim$100 cm^{-1}), sharpening to 0.25 nm ($\sim$5 cm^{-1}) in the absence of a tuning element. For cavity lengths of $\sim$25 cm, this takes place over 100 to several hundred microseconds. As the name denotes, ILS deals with the absorptions that occur when a species, whose absorption features lie in the emitted spectral region and are narrow enough to attenuate only a portion of the evolving broadband laser pulse, is present within the cavity. As the light resonates in the cavity, the total optical path through the absorber increases, resulting in an absorption enhancement by factors as high as 10^7 versus a single pass.[14] The cavity effectively serves as a multiple reflection cell where the total path length is proportional to the generation time t_g of the pulse, i.e., the elapsed time between when the dye laser reaches threshold and the observation of the laser emission spectral profile.

The advantages of ILS, in particular its high sensitivity and fast response time, have led to its use in a variety of applications, including the study of combustion processes,[15] the detection of free radicals,[16] the measurement of chemical rate constants,[17] and the detection of species in supersonically cooled jets.[18] Burakov[19] provides a comprehensive review of the development and applications of ILS. Numerous studies of the theoretical basis for ILS have also been published; however, there remains disagreement on the interpretation of the observed effects. Reviews by T. D. Harris,[20] S. J. Harris,[21] and Baev *et al.*[14] summarize the principal theories proposed to explain ILS and describe many of the earlier ILS experiments. Applications of ILS by use of dye lasers continue to appear, most recently in the measurement of CH_4 line parameters at low temperatures,[22,23] the detection of HCO radicals in hydrocarbon flames,[24] and the first suggestion that ILS be used to detect atmospheric trace species.[25] In addition, the suitability of titanium:sapphire and Cr^{4+}:YAG lasers for ILS has been demonstrated recently by Gilmore *et al.*[26,27]

Until now, ILS has been performed with some variant of the trigger/delay/scan-spectrum scheme with the time delay held fixed and a gated grating spectrometer or optical multichannel analyzer (OMA) recording the laser emission wavelength profile.[20] Because each scan records a spectrum for only one generation time, usually only one or a small set of time-delayed spectra were recorded. OMA systems have the advantage that the entire spectrum is recorded with each shot, and pulse-to-pulse variability can be averaged over many pulses; however, for the ILS application, the spectra must still be recorded sequentially, one for each generation time. Thus investigations of the dynamics of ILS, which require the acquisition of complete spectra at a series of generation times, can be time-consuming with OMA technology.

In contrast, in the step-scan TRS experiments, although the laser pulse has to be repeated for several mirror positions, the full desired time resolution of the evolving pulse is obtained at essentially no additional cost in terms of the duration of the experiment. In terms of the number of time slices, for example, once the laser pulse has been initiated, either one digitization at 5 μs or 100 digitizations at 5, 10, 15, . . . , 500 μs can be recorded with no difference in the resulting experiment time. This is because the evolution time (typically 500 μs) is essentially negligible relative to the step and stabilization time of the moving mirror (typically 50 ms); one can digitize as many or as few points as desired during this interval. A further point concerns the effect on the measurement time, not of the number of digitizations per laser pulse, but of the use of pulse averaging in-step to improve the signal-to-noise ratio (SNR). With such in-step averaging of a number of laser pulses N, while the mirror is fixed at one position, the SNR is increased as $\sqrt{N}$, with only a small increase in the total experiment time. There is, of course, a limitation to this—namely when the number of co-added laser pulses becomes comparable to the mirror step

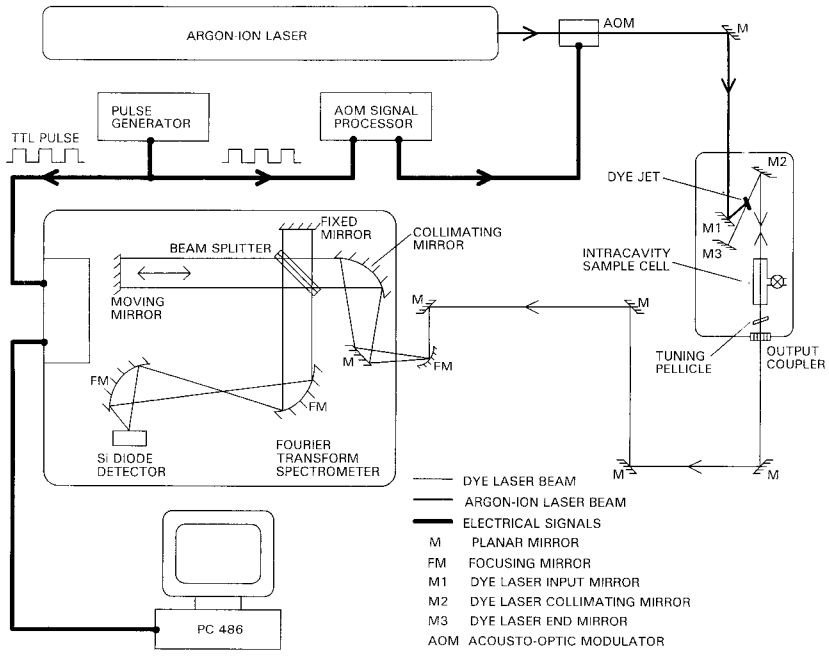

Fig. 1. Schematic diagram of the experimental apparatus. TTL, transistor–transistor logic.

and stabilization time. For the current system, with mirror translation times of ~50 ms and laser switching rates of ~1 kHz, approximately 50 laser pulses could be co-added before further pulse averaging became the dominating factor in the overall measurement time.

In our current research we apply step-scan FT techniques to the ILS experiment for the first time to our knowledge. The TRS method has the advantage of allowing the time evolution of the laser emission to be studied easily, enabling, for example, the straightforward determination of the generation time that yields the optimum intracavity absorption signal and accurate determination of the limits of linearity of the method. The long-term goal of these studies is to extend the step-scan TRS–ILS combination to wavelength regions (mid and near infrared) that are rich in atmospheric absorptions, but for which fast OMA devices are not readily available or simply do not exist.

2. Experiment

The experimental apparatus used in our experiment is depicted in Fig. 1. A Coherent Innova 90 argon-ion laser running on all lines at powers of approximately 1.5 W is used to pump the dye laser. The pump laser is intensity modulated by an IntraAction acousto-optic modulator (AOM) that is switched at ~1 kHz; when the AOM is switched on, the zero-order pump beam is transmitted at a lower power to maintain the dye laser just below threshold. The AOM-modulated beam pumps a Spectra-Physics 375B dye laser equipped with an ~3:1 mixture of Exciton Rhodamine 590 chloride (R6G) and Kiton Red laser dyes, yielding emission maxima at ~615 nm. For the CH_4 experiments reported below, a 2-μm tuning pellicle (National Photocolor) was used to tune the emission maximum to 619 nm. The emitted beam was expanded and focused into the emission port of a Bruker IFS 66v FT spectrometer equipped with a quartz beam splitter and a Si diode detector.

Figure 2 depicts the triggering scheme, whereby a square wave produced by a pulse generator turns off the AOM such that the full Ar^+ laser power appears in the zero order and simultaneously initiates the Fourier-transform infrared (FTIR) data acquisition at a given step. With the interferometer mirror held fixed, the intensity of the interferogram point is recorded and digitized at 10-μs intervals. To improve the SNR ratio, usually between 40 and 200, evolving

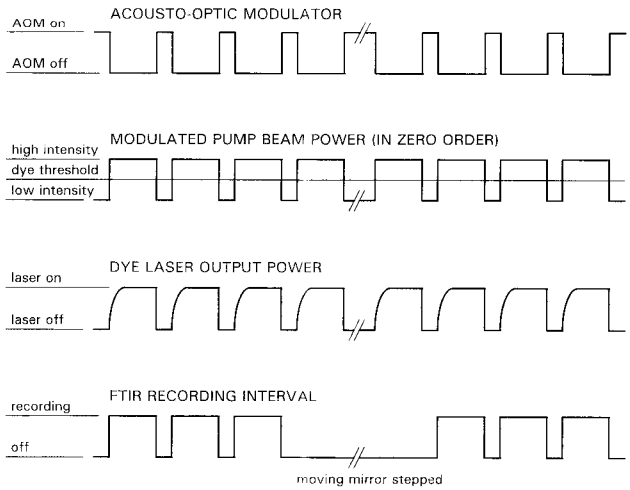

Fig. 2. Timing scheme for the FTIR–ILS experiment. An approximate switching time for the AOM is 1 ms with a 50% duty cycle.

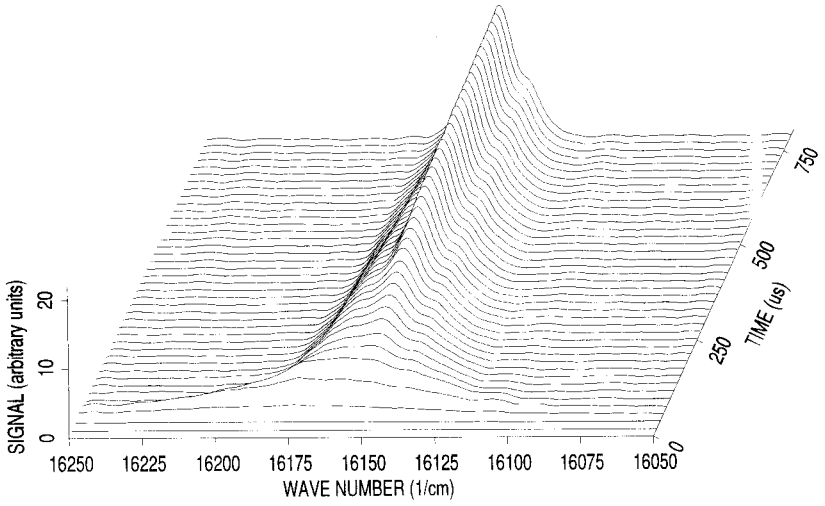

Fig. 3. Time-resolved spectra of the intracavity dye laser pulse for the N_2-purged cavity. The total Nyquist bandwidth was 1215 cm^{-1}, with a spectral resolution of 4.0 cm^{-1} and a temporal resolution (spacing between time slices) of 20 μs. Forty laser shots were averaged at each step.

laser pulses were digitized and averaged in-step (three such in-step averages are shown in Fig. 2); typical values for the SNR were ~100:1 to ~1000:1 or better, depending on the number of in-step averages and the generation time (and hence laser signal strength). After averaging, the interferometer mirror is moved to the next position, and the cycle is repeated until a complete two-dimensional intensity matrix of interferogram intensities and mirror positions is collected. The data are then transposed and Fourier transformed as described above. The complete acquisition time for a set of spectra covering a 1200-cm^{-1} Nyquist bandwidth at 1.0-cm^{-1} resolution is approximately 12 min; we typically stored 50 times slices, but this number can be selected arbitrarily with minimal effect on the overall acquisition time.

3. Results and Discussion

Figure 3 illustrates the advantage of performing ILS by the step-scan technique, namely that extensive spectral and temporal information are obtained within a single experiment. This figure presents time-resolved emission spectra of the dye laser pumped by the Ar^+ laser at 0.90 W, with the dye laser cavity purged by dry N_2. The spectral resolution is 4.0 cm^{-1} and the temporal resolution is 20 μs between the 50 slices displayed, for a total generation time of 1 ms. As can be seen, the pulse width narrows over the first few hundred microseconds as the pulse height grows. This particular series of spectra was obtained with 40 in-step averages. Because the dominant noise source originates from the dye laser (stochastic shot noise and pulse-to-pulse jitter[28,29]), further averaging improved the SNR, at least to the point where 200 in-step shots were averaged. Amplitude and frequency jitter in the output of the dye laser probably originate from flow instabilities, including bubbles, within the dye stream and seemed to worsen with extended running time.[30]

It is of interest to analyze the evolution of both the peak height and the width as a function of time, since there is currently no conclusive statement in the literature as to these relations. The development of the laser rate equations is rather involved, but we favor a model first developed by Burakov[19] and Antonov *et al.*[31] and more recently presented by Stoeckel and Atkinson.[32] This model assumes that there is no wavelength-dependent absorber within the cavity and that the gain curve for the mode distribution is represented by an inverted parabola of finite width. Making these assumptions, one arrives at the following relation for the laser intensity as a function of wave number and generation time:

$$I(\tilde{\nu}, t) = \frac{I_0'}{\Delta\tilde{\nu}_0}\left(\frac{\gamma t_g}{\pi}\right)^{1/2} \exp\left[-\left(\frac{\tilde{\nu}-\tilde{\nu}_0}{\Delta\tilde{\nu}_0}\right)^2 \gamma t_g\right], \quad (1)$$

where

I_0' = total laser intensity,
t_g = generation time,
γ = losses in the optical cavity,
$\tilde{\nu}$ = spectral frequency (cm^{-1})
$\tilde{\nu}_0$ = frequency at line center of laser gain profile (cm^{-1}), and
$\Delta\tilde{\nu}_0$ = initial bandwidth (cm^{-1}).

The second coefficient yields a peak height increasing in proportion to the square root of the generation time $\sqrt{t_g}$, whereas the exponential term dictates a half-width that is decreasing as $1/\sqrt{t_g}$. We took the peak heights and widths from the spectra in Fig. 3 and plotted their logarithms versus the logarithm of the generation time in Fig. 4. Clearly, for times ≥500 μs, Eq. (1) no longer holds, as the peak amplitude and peak width reach constant values, with the free-running dye laser operating on hundreds or even thousands of modes. The source of the limitation that terminates further change in the generation spectra (i.e., no further reduction in the number of

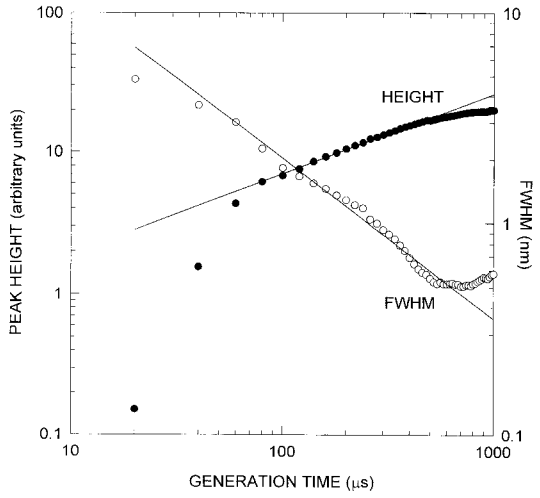

Fig. 4. Log–log plot of peak height (left axis) and spectral width (FWHM, right axis) versus generation time for the spectra shown in Fig. 3. The circles are the measured data and the solid curves are the fits to all points between 80 and 500 μs.

modes) has been the topic of much discussion. Spatial inhomogeneity plays a role,[14,21] but the primary limitation at shorter times (<1 ms) appears to be small changes in the refractive index of the cavity media, i.e., the dye and the cavity air, that lead to fluctuations in the optical path length of the cavity.[32] The data between 80 and 500 μs yield a slope for the logarithm of the peak height versus time of 0.57 and a slope for the logarithm of the FWHM versus time of −0.76. For the peak height, this is in reasonable agreement with Eq. (1), whereas the peak shape, and hence width, is less clearly defined. The large number of data points, which are conveniently obtained with the TRS–ILS technique, allows greater precision to the fit than has been obtained in previous studies and suggests that the evolution of the mode distribution may not be described satisfactorily by the exponential term in Eq. (1). Figure 3 also demonstrates a red shift as the generation time increases ($\Delta\tilde{\nu}$ = 27.3 cm^{-1}), as noted by others,[14,32,33] which is a further apparent shortcoming of Eq. (1). Stoeckel and Atkinson[32] showed that at least part of this effect is caused by fluctuations in the intracavity path length such as those caused by refractive-index changes. We suggest that the red shift may be due in part to the pulsed laser heating of the dye, changing the Boltzmann population of the dye and thus altering the gain curve during the course of the emission.

Our objective is to take advantage of the high sensitivities offered by the long equivalent path lengths at intermediate generation times and to apply the TRS–ILS method to atmospheric trace gas analysis in wavelength ranges where diode-array technology is impractical; in this paper we verify the feasibility and investigate the performance of step-scan TRS–ILS in the visible region. To this end, the 619.68-nm overtone line of CH_4 was selected, as its line strength and pressure-broadening coefficients have been determined previously.[22,34] A windowless cell, 91.5 mm long with a 4.9-mm inner diameter, was placed within the dye laser cavity and flushed with a continuous flow of 30 SCCM 99% pure CH_4. (SCCM denotes cubic centimeter per minute at STP.) The cell served to direct the flow coaxially with the laser beam inside the cavity. Before an experiment, the CH_4 was flowed for a sufficient time to flush the entire dye laser housing. Although the housing is not completely airtight, we estimate that, of the total 36-cm optical path within the dye laser, a equivalent length of at least 30 cm was occupied by CH_4 at atmospheric pressure. To center the dye laser emission profile near the absorption line, a 2-μm tuning pellicle was also placed just before the output coupler within the cavity.[22] For this experiment, the Ar^+ laser power was 1.5 W and the AOM was switched at 1.3 kHz. During step-scan acquisition, spectra were recorded at 10 generation times at 20-μs intervals with 100 in-step averages.

The results of the experiment are displayed in Fig. 5(a) as a stacked plot of the emission profile as a function of time. The bandwidth covered was

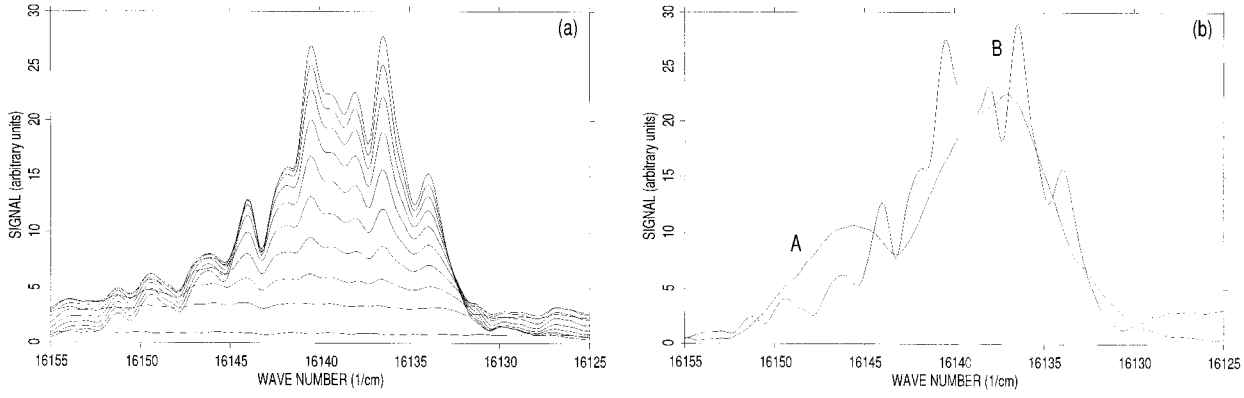

Fig. 5. (a) Time evolution of the ILS pulse through CH_4. The displayed slices range from 0 to 180 μs at 20-μs intervals. (b) Comparison of the 190-μs time slices for the ILS experiment: Curve A is for N_2 in the cavity and curve B is for CH_4. See text for details.

15,800–16,800 cm^{-1} at 0.5-cm^{-1} apodized resolution, with the time slices corresponding to generation times of 0–180 μs. The spectra shown are the averages of eight spectra, post-run extracted for each generation time from eight independent step-scan experiments. Each spectrum was recorded in 15 min, so that 2 h of total instrument operation time were required to record the set of eight spectra. As a control experiment, the CH_4 was replaced by a 40-SCCM flow of pure N_2. The ILS traces for CH_4 and N_2 at t_g = 190 μs are juxtaposed in Fig. 5(b), showing that, whereas some of the structure is due to the characteristics of the laser and acquisition system rather than to intracavity absorptions, the prominent feature at 16,137.3 cm^{-1} is the well-known CH_4 overtone line. Much of the additional spectral congestion arises from other CH_4 absorptions.[22] The pressure self-broadening coefficient γ_s of this line at 296 K was measured to be 0.138 cm^{-1}/atm.[22] Thus the line is underresolved by approximately a factor of 3 at our resolution, but since the maximum apparent spectral contrast is only ~20%, optical saturation can be neglected even at the longest generation times used in this experiment.

The temporal behavior of the CH_4 absorption spectrum can be understood in terms of accepted ILS theory. The relation governing optical attenuation in an ILS spectrum is given by[32]

$$\frac{I}{I_0} = \exp\left[-\alpha(\tilde{\nu})\frac{l}{L}ct_g\right], \tag{2}$$

where $\alpha(\tilde{\nu})$ is the extinction coefficient at wave number $\tilde{\nu}$, l is the length of the gas cell in a total cavity of length L, c is the speed of light, and I and I_0 represent the intensity of the spectra with and without the absorber, respectively. This is similar to the Beer–Lambert relation for optical absorption with the path length replaced by the term ct_g, scaled by the term l/L to account for the absorber not filling the entire dye laser cavity. Briefly, the longer the generation time, the more traversals of the light through the sample and the longer the effective path length.

To test this relation, we calculated $\ln(I_0/I)$ at 16137.3 cm^{-1} for the series of generation spectra through the CH_4 sample. For each spectrum, a baseline was drawn between the two adjacent maxima (at 16,136.0 and 16,138.4 cm^{-1}) to calculate the corresponding I_0. Figure 6 shows the calculated optical depth versus the generation time t_g between 20 and 180 μs, which yields an approximately linear relationship with a correlation coefficient of r^2 = 0.994. Careful inspection of the plot shows that the curve is starting to deviate from linearity at longer generation times. The pseudo Beer–Lambert law behavior predicted by Eq. (2) arises from a simplified model of ILS that apparently is reasonably valid for small absorptions. At longer generation times (larger optical densities), other effects alter the distribution of energy among cavity modes and influence the emission profile in ways that are difficult to treat theoretically. The data in Fig. 6 demonstrate the

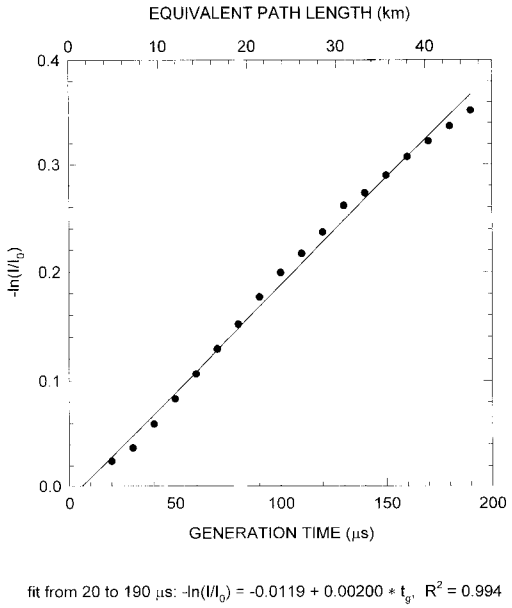

Fig. 6. Plot of $\ln(I_0/I)$ versus generation time t_g for the 16,137.3-cm^{-1} CH_4 absorption line shown in Fig. 5. See text for details.

advantage of recording data at a large number of generation times, which is facile in the step-scan TRS–ILS method, to provide a measure of the limit of applicability of the linear pseudo Beer–Lambert relationship. As discussed above, the multiple time slices are obtained effectively with no increase in the requisite measurement time.

It is of interest to consider the performance of step-scan TRS–ILS compared with traditional methods with use of a gated OMA in terms of minimum detectable spectral contrast. However, the issue is rather complex since the two techniques are inherently different in how the data are obtained. For dispersive systems using OMA registration, the considerations are straightforward. In such systems the entire spectrum of the pulse is observed at one fixed generation time in each experiment, and averaging over many pulses can be done directly (on chip). Thus, since pulse-to-pulse variability is stochastic, signal recovery improves with the square root of the number of pulses averaged per generation time.

Similar considerations for the step-scan ILS are somewhat more complex. In the simplest case in which just one laser pulse is used at each mirror position, each spectrum, obtained after the transformation of the sets of interferograms, contains information from every laser pulse. A single aberrant pulse, which in the equivalent normal ILS experiment would corrupt just one generation time, introduces correlated distortion into every interferogram in the TRS–ILS method, and the severity of the distortion is a function of the particular step (mirror retardation) at which the aberrant pulse occurred. In practice, many laser pulses are averaged at each step, reducing the importance of variability between individual pulses. The practical considerations concerning the number of in-step averages selected re-

late to the maximum generation times required (which limits the repetition rate of the pump laser) and the settling time for the moving mirror to be stabilized at its new position after a step (which determines the minimum time required to obtain a set of step-scan spectra without in-step averaging). For example, the present FTIR has a mirror translation and settling time of ~35 ms, and if we wish to observe generation times to 500 μs, the modulation of the AOM must be limited to ~1.5 kHz. Thus, for example, 50 shots (requiring ~33 ms) can be averaged per step, approximately doubling the total duration of the experiment compared with the single-shot case but improving the SNR of each interferogram by $\sqrt{50}$ or ~7. For clarity, we reiterate that there is no effect on acquisition time if only one or as many as 100 time slices are recorded to the desired 500-μs maximum generation time. Nonetheless, the effect of noise in the interferograms, introduced by pulse-to-pulse amplitude variability, on the transformed spectra will be correlated for all selected generation times, and the effect on minimum retrievable spectral contrast for a particular ILS experiment is difficult to generalize. Thus, although a direct theoretical comparison between TRS–ILS and diode array systems is not straightforward, it appears that for comparable conditions (e.g., 1000-cm^{-1} bandwidth at 0.5-cm^{-1} resolution) a 30-min step-scan ILS experiment yields spectra that are of comparable quality to those illustrated in the literature. We note again that all the data points shown in Fig. 6 can be derived from a single 30-min experiment.

The enhancement factor obtained in ILS relative to a single pass through the cavity can be derived by an estimation of the path length according to $ct_g l/L$. At 200 μs we obtained a total path of 60 km and a single-path distance of ~30 cm, yielding an enhancement of $\sim 2 \times 10^5$. We performed a further test of the sensitivity in the current system by subtracting spectra at the same t_g for two independently acquired (and hence uncorrelated) sets of spectra. The amplitude of the resulting rms noise thus represents a figure for the minimum detectable spectral contrast. This was found to be ~0.01 to ~0.06 (units of optical depth) for generation times in the range from 60 to 200 μs (i.e., equivalent absorption path lengths of 20–60 km), an encouraging result for the detection of trace gas species.

4. Summary

We have demonstrated ILS using an Ar^+-pumped dye laser together with a step-scan FT spectrometer. This novel approach allows the combination of high spectral (e.g., <0.5-cm^{-1}) and temporal (as high as 5-μs) resolution in a manner that can decrease significantly the requisite acquisition time when several generation times are being investigated. For our system, we observed predicted behavior of the pulse characteristics for generation times as high as 500 μs, depending on the conditions under which the experiment was run. ILS studies using the 619.68-nm CH_4 overtone line were consistent with literature reports using dye lasers, and we have shown that our method allows easy determination of the linear range in the absorption (spectral contrast) for the CH_4 line as a function of generation time. In general, provided that the species of interest have a relatively narrow absorption feature at a wavelength to which an open cavity laser can be tuned, the system shows promise for the sensitive detection of atmospheric trace species. Use of a closed gas cell in the laser cavity will require careful consideration of the window dimensions and orientation, as the windows act as tuning elements in the system. Atmospheric applications of the ILS technique is the focus of current research in our laboratories.

T. J. Johnson thanks G. H. Atkinson of the University of Arizona for helpful clarification of several experimental points. The authors also thank B. McManus of Aerodyne Research for helpful discussions and the referee of an earlier version of this paper who pointed out the problem of optical saturation in initial experiments when I_2 is used as the absorber.

References

1. B. A. Garetz and J. Lombardi, eds., *Advances in Laser Spectroscopy*, Vol. 2 (Wiley, New York, 1983).
2. P. R. Griffiths, *Chemical Infrared Fourier Transform Spectroscopy* (Wiley, New York, 1975).
3. P. Biggs, G. Hancock, D. Heard, and R. P. Wayne, "A stop-scan interferometer used for time-resolved FTIR emission spectroscopy," Meas. Sci. Technol. **1,** 630–636 (1990).
4. G. Hancock and D. E. Heard. "Time-resolved pulsed FTIR emission studies of atom-radical reactions: product chemiluminescence from the $O(^3P) + CF_2(X^1A_1)$ reaction," Chem. Phys. Lett. **158,** 167–171 (1989).
5. R. A. Palmer, C. J. Manning, J. A. Rzepiela, J. M. Widder, and J. L. Chao, "Time-resolved spectroscopy using step-scan Fourier transform interferometry," Appl. Spectrosc. **43,** 193–195 (1989).
6. G. V. Hartland, W. Xie, H.-L. Dai, A. Simon, and M. J. Anderson, "Time-resolved Fourier transform spectroscopy with 0.25 cm^{-1} spectral and $<10^{-7}$ s time resolution in the visible region," Rev. Sci. Instrum. **63,** 3261–3267 (1992).
7. G. V. Hartland, D. Qin, and H.-L. Dai, "Fourier transform dispersed fluorescence spectroscopy: observation of new vibrational levels in the 5000-8000 cm^{-1} region of $\tilde{a}\ ^1A_1\ CH_2$," J. Chem. Phys. **98,** 2469–2472 (1993), and references therein.
8. T. J. Johnson, A. Simon, J. M. Weil, and G. W. Harris, "Applications of time-resolved step-scan and rapid-scan FT-IR spectroscopy: dynamics from ten nanoseconds to ten seconds," Appl. Spectrosc. **47,** 1376–1381 (1993).
9. W. Uhmann, A. Becker, C. Taran, and F. Siebert, "Time-resolved FT-IR absorption spectroscopy using a step-scan interferometer," Appl. Spectrosc. **45,** 390–397 (1991).
10. W. Hage, M. Kim, H. Frei, and R. A. Mathies, "Protein dynamics in the bacteriorhodopsin photocycle: a nanosecond step-scan FTIR investigation of the KL to L transition," J. Phys. Chem. **100,** 16026–16033 (1996), and references therein.
11. S. Plunkett, J. L. Chao, T. J. Tague, and R. A. Palmer, "Time-resolved step-scan FTIR spectroscopy of the photodynamics of carbonmonoxymyoglobin," Appl. Spectrosc. **49,** 702–708 (1995).
12. C. Peterson, M. J. Kurylo, W. Braun, A. M. Bass, and R. A. Keller, "Enhancement of absorption spectra by dye-laser quenching," J. Opt. Soc. Am. **61,** 746–750 (1971).
13. A. Pakhomycheva, E. A. Sviridenkov, A. F. Suchkov, L. V.

Titova, and S. S. Churilov, "Line structure of generation spectra of lasers with inhomogeneous broadening of the amplification," JETP Lett. **12,** 43–45 (1970).
14. V. M. Baev, I. N. Sarkisov, E. A. Sviridenkov, and A. F. Suchkov, "Intracavity laser spectroscopy," J. Sov. Laser Res. **10,** 61–85 (1989).
15. J. Thrash, H. von Weyssenhoff, and J. S. Shirk, "Dye laser amplified absorption spectroscopy of flames," J. Chem. Phys. **55,** 4659–4660 (1971).
16. H. Atkinson, A. H. Laufer, and M. J. Kurylo, "Detection of free radicals by an intracavity dye laser technique," J. Chem. Phys. **59,** 350–354 (1973).
17. H. Clark, C. B. Moore, and J. P. Reilly, "HCO radical kinetics: conjunction of laser photolysis and intracavity dye laser spectroscopy," Int. J. Chem. Kinet. **10,** 427–431 (1978).
18. N. Goldstein, T. L. Brack, and G. H. Atkinson, "Quantitative absorption spectroscopy of NO_2 in a supersonically cooled jet by intracavity laser techniques," Chem. Phys. Lett. **116,** 223–230 (1985).
19. V. S. Burakov, "Development of intracavity laser spectroscopy," J. Appl. Spectrosc. **35,** 843–854 (1981).
20. T. D. Harris, "Laser intracavity-enhanced spectroscopy," in *Ultrasensitive Laser Spectroscopy*, D. S. Kliger, ed. (Academic, New York, 1983), pp. 343–367.
21. S. J. Harris, "Intracavity laser spectroscopy: an old field with new prospects for combustion diagnostics," Appl. Opt. **23,** 1311–1318 (1984).
22. P. V. Cvijin, W. K. Wells, I. Mendas, J. K. Delaney, J. I. Lunine, D. M. Hunten, and G. H. Atkinson, "Determination of line intensity and pressure broadening of the 619.68 nm methane overtone absorption line at low temperatures using intracavity laser spectroscopy," J. Quant. Spectrosc. Radiat. Transfer **49,** 639–650 (1993).
23. B. B. Radak, J. I. Lunine, D. M. Hunten, and G. H. Atkinson, "The intensity and pressure broadening of the 681.884 nm methane absorption line at low temperatures determined by intracavity laser spectroscopy," J. Quant. Spectrosc. Radiat. Transfer **52,** 809–818 (1994).
24. S. Cheskis, "Intracavity laser absorption spectroscopy detection of HCO radicals in atmospheric pressure hydrocarbon flames," J. Chem. Phys. **102,** 1851–1854 (1995).
25. J. B. McManus and C. E. Kolb, "Long-path intracavity laser for the measurement of atmospheric trace gases," in *Measurement of Atmospheric Gases*, H. I. Schiff, ed., Proc. SPIE **1433,** 340–351 (1991).
26. D. A. Gilmore, P. V. Cvijin, and G. H. Atkinson, "Intracavity absorption spectroscopy with a titanium:sapphire laser," Opt. Commun. **77,** 385–389 (1990).
27. D. A. Gilmore, P. V. Cvijin, and G. H. Atkinson, "Intracavity laser spectroscopy in the 1.38-1.55 μm spectral region using a multimode Cr^{4+}:YAG laser," Opt. Commun. **103,** 370–374 (1993).
28. V. R. Mironenko and V. I. Yudson, "Quantum noise in intracavity laser spectroscopy," Opt. Commun. **34,** 397–403 (1980).
29. M. Chenevier, M. A. Melieres, and F. Stoeckel, "Intracavity absorption line shapes and quantitative measurements on O_2," Opt. Commun. **45,** 385–391 (1983).
30. S. J. Harris and A. M. Weiner, "Continuous wave intracavity dye laser spectroscopy. II. A parametric study," J. Chem. Phys. **74,** 3673–3679 (1981).
31. E. N. Antonov, A. A. Kachanov, V. R. Mironenko, and T. V. Plakhotnik, "Dependence of the sensitivity of intracavity laser spectroscopy on generation parameters," Opt. Commun. **46,** 126–130 (1983).
32. F. Stoeckel and G. H. Atkinson, "Time evolution of a broadband quasi-cw dye laser: limitations of sensitivity in intracavity laser spectroscopy," Appl. Opt. **24,** 3591–3597 (1985).
33. V. M. Baev, T. P. Belikova, S. A. Kovalenko, E. A. Siridenkov, and A. F. Suchkov, "Transient processes manifested in the emission spectra of c.w. wide-band dye lasers used for intracavity laser spectroscopy," Sov. J. Quantum Electron. **101,** 517 (1980).
34. P. V. Cvijin, J. J. O'Brien, G. H. Atkinson, W. K. Wells, J. I. Lunine, and D. M. Hunten, "Methane overtone absorption by intracavity laser spectroscopy," Chem. Phys. Lett. **159,** 331–336 (1989).